

Theory and design of an ultrasound loudspeaker

C. Gallardo, J. Gosálbez, Alicia Carrión, Ramón Miralles, Ignacio Bosch, Guillermo Lara, Guillermo Pérez, Santiago Vazquez

Instituto de Telecomunicaciones y Aplicaciones Multimedia,
Universitat Politècnica de València,
8G Building, access D - Camino de Vera s/n - 46022 Valencia (Spain)
Corresponding author: cargall2@teleco.upv.es

Abstract

The design of directive loudspeakers is a challenge for traditional techniques because it implies big speakers due to the sound wavelength. In this work, the design of a directive loudspeaker using PZT ultrasound transducers is presented. This technique uses lineal modulation between ultrasound carrier signal and acoustic message and takes advantage of non-linear propagation effects. These non-linear effects produce intermodulation phenomena between ultrasonic carrier frequency and transmitted signal demodulating and generating an audible and very narrow beam on the pointing direction of ultrasound loudspeaker. In this work, the theoretical aspects, the critical factors and a real implementation of this technique are presented.

Keywords: Ultrasonic loudspeaker, Parametric Acoustic Array, directional beam, sound beam, non linear ultrasound effects.

1. Introduction

It is well-known that modern loudspeakers do not radiate the sound equally in all directions. The directivity of a loudspeaker is defined as the main direction which the acoustic power produced by a loudspeaker is radiated [1]. To quantify this directivity, the ratio between the acoustic intensity at a given point of an imaginary sphere surrounding the loudspeaker and the total transmitted energy is calculated. In order to reduce the measuring time and to simplify the measures, the experimental is carried out along one plane [2].

If we want to increase the directivity of conventional speakers, one solution is to make the speakers of several meters of diameter due to the audio wavelengths or to make speaker arrays, which are also big and it is impractical to carry them out [3]. Therefore, if we want to increase the directivity with a reduced

size, we should increase the frequency in order to reduce the wavelength. Above 16 kHz, the beam is not longer audible to humans and above 30 kHz we can consider that we are already in the band of ultrasounds. It is in this band where the concept of ultrasonic loudspeaker appears, with only 20 cm in diameter is able to achieve a directivity similar to that made by large speakers [3]. We obtain a very directive beam because the ultrasound frequencies are higher than acoustic frequencies and have much shorter wavelengths. However, this signal would be completely inaudible for humans since their bandwidth frequency is above the audible range. To solve this problem, the ultrasonic signal is linear modulated by an acoustic signal. When the ultrasound signal propagates through the air, with a high amplitude level (greater than 110 dB_{SPL} [4]), a nonlinear effect occurs. This effect demodulates the signal and produces a directional beam, but now, in the audible range, along with the ultrasound beam of the modulated signal. This kind of ultrasound speakers is also known as PAA (Parametric Acoustic Array) because its propagation characteristics depend on different variables or parameters.

The aim of this work is the development of a unidirectional loudspeaker with a radiation pattern much more directive than conventional loudspeakers. Specifically, we will focus to obtain a loudspeaker with a radiation pattern less than 10° that will allow sending messages to a specific point. The remainder of this work is organized as follows. Section 2 presents the basics of parametric theory that will condition the design. In Section 3, the hardware implementation of a PAA is presented considering the theoretical aspects and technical specifications of the devices. In Section 4, some results of the implemented PAA are presented and compared with theoretical concepts. Finally, the last section contains the main conclusions of the parametric design.

2. Theory of the parametric loudspeaker.

2.1. Introduction

A parametric acoustic array (PAA) consists of a cluster of ultrasonic transducers that emit an ultrasonic signal which is linearly modulated by an audio signal. When the transmitter carries out the transmission of this modulated signal over the linear limits (ULN) (around 110 dB_{SPL} [4][3]), the non-linear effects in the air are produced, creating intermodulation effects and an auto-demodulation of the audio signal. This fact occurs because the air in front of the emitting source acts as a virtual end-fire volumetric array, then the air molecules oscillate at audio frequency and become as a virtual source of sound generating a secondary and audible directional beam in the same direction of the primary ultrasound beam (Figure 1). This array has an effective array length, also called absorption length, which indicates the attenuation of the pressure level of the higher frequencies (primary waves). This length is considered as the end of the non-linear interaction and it is necessary to take into account for the design of the speaker (Section 3). For now, we can assume that this distance is a function of the combined absorption losses.

In Figure 1, the two beams are shown; the primary one, which is formed by the ultrasound carrier and its envelope (AM modulation) and the secondary one, which is formed by audible frequencies.

The primary beam (ultrasound beam) is absorbed before than the audible one because the absorption increases with distance and frequency. Therefore, the secondary beam (audible beam) is the one that can cross certain distance and is also called "difference" because its generation is due to intermodulation effect. The intermodulation effect¹ is considered between the two tones, but the same effect is applicable for an amplitude modulated signal and it generates upper band (double of carrier frequency) and lower band (audible message) of the primary waves. Apart from the desired audible message (lower band), unwanted harmonics also are originate, as we can see in [5]. Therefore, the reduction of harmonic distortion and distortion of cross modulation is significant in the design of the parametric loudspeakers.

In order to get an idea how directional and narrow will be the secondary beam (audible beam), we resort to [6], which states that when two primary frequency waves f_1

and f_2 ($f_2 > f_1$) are confined to two beams, the beamwidth (-3dB), Θ_n , for the frequency difference $f_2 - f_1$ is given by equation (1)

$$\Theta_n \approx \sqrt{\frac{2\alpha_T}{k}} \quad (1)$$

where k is the wave-number of the difference frequency and α_T is the overall absorption of the primary wave. When $f_1 \approx f_2$, $\alpha_T \approx 2\alpha_1$, we can rewrite equation (1) as equation (2), where α_1 is the coefficient of absorption of primary wave of frequency f_1 .

$$\Theta_n \approx \sqrt{\frac{2\alpha_T}{k}} = \sqrt{\frac{4\alpha_1}{k}} = \sqrt{\frac{4\alpha_1 c}{2\pi f_d}} \quad (2)$$

According to equation (2), directivity of the secondary beam is independent of the aperture of the source, on the contrary of linear theory, which shows that directivity of the primary beam depends on two main parameters, carrier frequency (carrier) and the opening of the source. Strictly, the primary beam depends on the aperture, especially when the wave difference is comparable or smaller than the aperture. As an example, if we assume that the primary frequency is 40 kHz, the frequency difference is 2 kHz and the attenuation coefficient for air is 0.15 Neper/m at 40kHz under normal condition. Therefore, applying equation (2), we will obtain that Θ_n is 7.4°. However and according to the linear theory, a very large aperture speaker of at least 68 cm of radius would be required to obtain a similar beamwidth for 2 kHz [6].

In conclusion, the two important properties for parametric arrays are:

A very narrow and directional beam is obtained for low frequencies.

Significantly reduced lateral side lobes

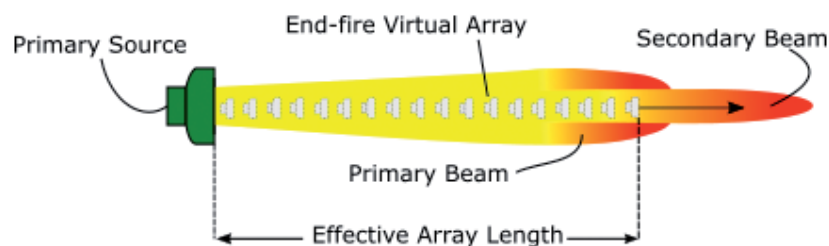
2.2. Non-linear effects: Berkta's Equation

In this section, we describe the Berkta's approximation [7] which is a more detailed study of the intermodulation effects and their dependence with carrier frequency, modulator frequency and distance. Berkta assumed that the primary wave had the following form:

$$P_1(t) = P_1 E(t) \sin(\omega_c t) \quad (3)$$

where $\omega_c = 2\pi f_c$ is the carrier pulse, $E(t)$ is the arbitrary envelope and P_1 refers to the part of the amplitude of the carrier that will be converted to sound pressure. It is

¹The intermodulation effect occurs when two sinusoidal ultrasound tones are radiated (f_1 and f_2), and two new waves are produced, whose frequencies are $f_d = f_1 \pm f_2$. f_d is the addition and subtraction frequency of the original frequencies, f_1 and f_2 .



■ **Figure 1.** Generation of the audible beam through the PAA.

therefore established for a point along the axial axis of radiation of the array that the secondary (or demodulated) beam is equation 4 [6][7]:

$$P_2(t) = \frac{\beta P_1^2 S}{16\pi\rho_0^{T,P} (c_0^T)^4 c_0^{T^4} z \alpha} \frac{\partial^2}{\partial t^2} E^2(\tau) \quad (4)$$

where P_1 is carrier frequency pressure, corresponding to the primary source; S is the area of the emitter, which is considered as the effective area of the transducer array; β is the coefficient of nonlinearity; $P_0^{T,P}$ is the density of air that depends on temperature, T , and sound pressure, P ; c_0^T is the small signal propagation velocity; α is the absorption coefficient or attenuation of the ultrasonic carrier and finally $\tau = t - \frac{z}{c_0^T}$, includes the time, t , and the time delay, $\frac{z}{c_0^T}$, that the wave takes to reach a certain distance, z , on the propagation axis.

This is the reason because it is called parametric acoustic array: the secondary beam or demodulated signal depends on four parameters:

- Carrier pressure (primary wave).
- Size of the ultrasonic source.
- Modulated signal envelope.
- The absorption coefficient that depends on the frequency of the ultrasonic carrier used for each case.

In this way, we can improve the quality and the sound pressure level of the audible signal modifying one of these four parameters. As example, the higher frequency, the higher absorption coefficient, and therefore we could improve the amplitude of the sound reducing the carrier frequency.

Additionally, another expression for $P_2(t)$ can be obtained from [3] as it is shown in equation (5) which clearly indicates the proportionality of the pressure with the previous parameters:

$$P_2 \propto \frac{P_c S_0 f_A^2 L_G}{z} \quad (5)$$

With P_c as the initial pressure level of the carrier, S_0 is the circular area of the emitter, f_A is the frequency of the modulating signal, x is the distance from the user to the ultrasonic loudspeaker and L_G is the effective length obtained from several aspects. Equation (5) shows that the pressure of the acoustic beams depends on the square of the frequency, f_A . This means a positive slope of 12 dB / octave. Therefore, it becomes necessary to equalize the audio signal before being introduced into the corresponding modulator.

Another model that evaluates the generated sound is the Model KZK (Khokhlov-Zabolotskaya-Kuznetsov), which calculates the pressure taking into account the nonlinearities produced in the primary waves (ultrasound waves), due to absorption and attenuation. It is the most useful and traditional method, combining nonlinearities, dissipation and diffraction of the directional sound beam. There are two techniques to solve it. The first one is the frequency domain called the spectral method. The problem of this method is the required computational time due to calculations related to shock waves, and therefore the formation of a substantial amount of a high

Audible pressure depends on carrier pressure, effective area, signal envelope and the absorption coefficient.

number of harmonics. Although they may be reduced [1,2].

2.3. Rayleigh distance, effective length and generation length

As it has been explained in Section 2.2, the parametric array theory describes the nonlinear interaction in the near field, but nonlinearities still occur beyond this zone, in the far field, producing different results. In this section, we will explain in more detail the concept of Rayleigh distance, effective length generation length and how their pairing can influence the design of the speaker.

2.3.1. Rayleigh distance

Westervelt described the parametric arrays by introducing the second-order wave equation. It also dealt with a quasi-linear solution, where there is a linear term (P_1) and a non-linear correction (P_2):

$$P = P_1 + P_2 \quad (6)$$

Berktay complemented this approach with a far-field solution for pressure difference and he considered a strong absorption. Therefore the nonlinearities should remain only in the near field.

The parameter describing the transition between the near and far field is known as *Rayleigh distance* and it is defined by as follows (equation 7):

$$z_0 = \frac{S}{\lambda} \quad (7)$$

where λ is the wavelength of the main frequency of the two primary waves (for us it is the carrier frequency) and S is the area of the source.

2.3.2. Effective length or Absorption length

The strong absorption condition is given by [8] where α_0 is the coefficient of absorption at the carrier frequency (ultrasound frequency).

$$\alpha_0 z_0 \geq 1 \quad (8)$$

In the case of our array, it is the total absorption coefficient that determines the extent of the interaction of nonlinearities [8] and it is a combination of different coefficients (equation 9),

$$\alpha_T = \alpha_a + \alpha_b + \alpha_- \quad (9)$$

where α_a and α_b are the coefficients of absorption of the primary frequencies and α_- is the absorption coefficient of the difference wave. Because the absorption coefficient of the difference wave is much smaller than that of the primary waves, we can disregard it, and the equation 9 simplifies to equation 10:

$$\alpha_T = 2\alpha_a = 2\alpha \quad (10)$$

Rayleigh distance should be matched to absorption length to obtain a high level of audible demodulated signal.

The effective length or absorption length indicates a significant decrease in the sound pressure level of the high frequencies. In fact, the end of the non-linear interaction is considered. Therefore, we can define the *absorption length* or *effective length* of the parametric array as (equation 11):

$$l_{ef} = l_a = \frac{1}{\alpha_T} = 1/2\alpha \quad (11)$$

As the quasi-linear approximation is used, the formation of shock waves does not take place in the array. The high absorption condition states that the Rayleigh distance must be longer than the absorption length, as we can see in Figure 2. For cases where the absorption length is greater than the Rayleigh distance, the generation of nonlinearities continues beyond the far field, producing an anticipated attenuation of the audible difference wave[9].

In [9], they propose a design criterion in which the length of absorption is compared to the Rayleigh distance, using one of the following methods. Increase the operating frequency to the lower the absorption length or increase the area of the ultrasonic source by increasing the Rayleigh distance. The first option is useful when speaker coverage needs to be shorter, such as in the case of a museum or in videogames. This will require the use of a different type of transducer having a higher resonant frequency. The second option, it becomes necessary to use a larger number of transducers, reaching a greater coverage distance. The advantage is that it is not required increasing the frequency and therefore the same type of transducers can be used.

2.3.3. Generation length

Another important parameter is the *Generation length*, described in [4]. The audible beam width is defined by the aperture of the source and the generation length (L_G) in terms of beam width and auditory volume, as we have seen in the previous sections. The directivity, as we will see below, depends on the distance to the emitter and its opening: a large active area gives a smaller beam width. For $x \leq L_G$ the beam width decreases as we approach the source. For $x \geq L_G$, the beam width remains constant. On the other hand, the generation length

depends on spherical propagation, dissipation and saturation. All effects that depend on the frequency and giving three characteristic lengths. This theory is very similar to the one commented on in the section of effective length but with certain margins of security as to the definitions of these three distances.

In the far-field region, where the listener's position is greater than the Rayleigh distance, the carrier's NPS begins to decrease gradually until it reaches a value below the ULN due to spherical propagation and the contributions generated can be considered negligible compared with which they are generated in the near field. Therefore, if we define that distance L_R as the distance where the carrier's NPS drops 3dB below its value to the Rayleigh distance, its definition would be as follows (equation 12):

$$L_R = \frac{\sqrt{2}S_0}{c_0} f_c \quad (12)$$

where f_c is the carry frequency. Similarly the L_D is defined as the dissipation distance where the NPS falls 3 dB below its initial value due to the atmospheric absorption corresponding approximately to (equation 13):

$$L_D = \frac{3}{c_0} \alpha(f_c) \quad (13)$$

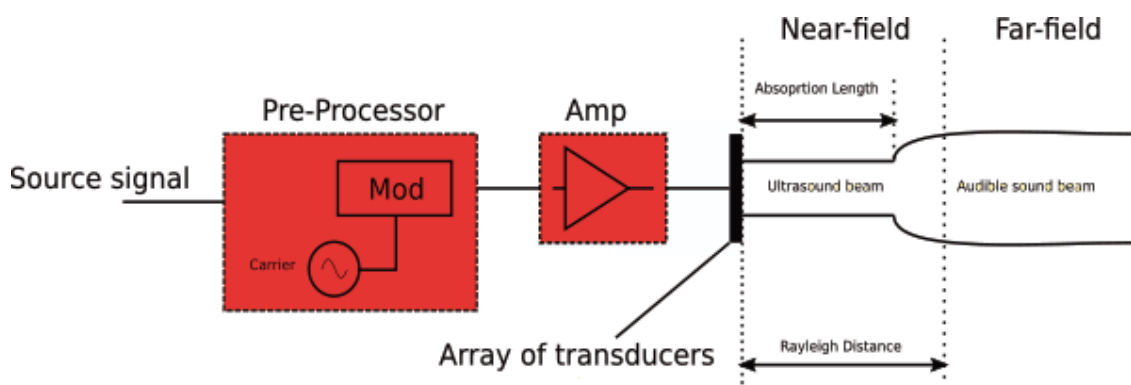
The remaining length to be determined is the acoustic saturation. It is established at a distance where there is an extra increase in the electric power level, which results in an increase in the level of harmonics of the carrier but not in its level. At three times this distance, the sawtooth shape is reached and the SPL decreases as we increase the distance. L_S denotes the distance where the NPS of the carrier falls approximately 3dB below its maximum value where it reaches the sawtooth shape (equation 14).

$$L_S = \frac{3 \rho_0 c_0^3}{\sqrt{2} \beta P_c f_c} \quad (14)$$

With only one effect of the previous ones occurring, L_G must be evaluated by the minimum of the three characteristic lengths (equation 15):

$$L_G = \min \{L_R, L_D, L_S\} \quad (15)$$

Although the frequency response is theoretically characterized by a slope of 12 dB / octave that produces an NPS drop at low frequencies, there is also an



■ **Figure 2.** Scheme of the loudspeaker system and regions of acoustic fields produced.

additional effect, the coherence length, which determines the lowest audible frequency that the speaker is capable of demodulating. To ensure a sufficient level at low frequencies and to take into account the slope, we set the low frequency objective limit two octaves above the lowest frequency and define that length as (equation 16):

$$L_c = \frac{2c}{f_{A,L}} \quad (16)$$

L_G should match the value of L_C .

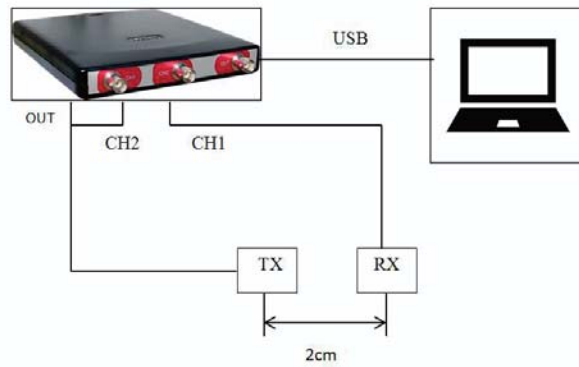
2.3.4. Conclusions

As a final recommendation at [9], it is suggested to match the Rayleigh distance to the absorption length to obtain an audible demodulated signal with a high level of pressure in the far field. They also add that future speaker designs would have to raise the possibility of expanding the Rayleigh distance beyond the length of absorption to obtain better results on the PAA and that if the high absorption condition is not met the theory should be reviewed to describe precisely how the PAA behaves in the far field.

All this serves as a design tool for choosing the fc according to the application you want to search. If an application is searched for meetings or encounters, a larger area with a smaller carrier NPS will be searched, the saturation limit being not restrictive in general for this case [4]. Conversely, if we want a shorter environment, we have to reduce the size of the emission surface at the expense of increasing the power of the carrier and its frequency.

3. Implementation

In this section, a real implementation of the PAA is explained taking into account the theoretical aspects described previously. For this purpose, this section is composed by 4 subsections. The first one describes the study of ultrasonic transducers based on their sensibility. Section 3.2 describes the chosen shape of the PAA to perform an optimal active surface. Finally, sections 3.3 and 3.4 describe the layout and the amplifier.



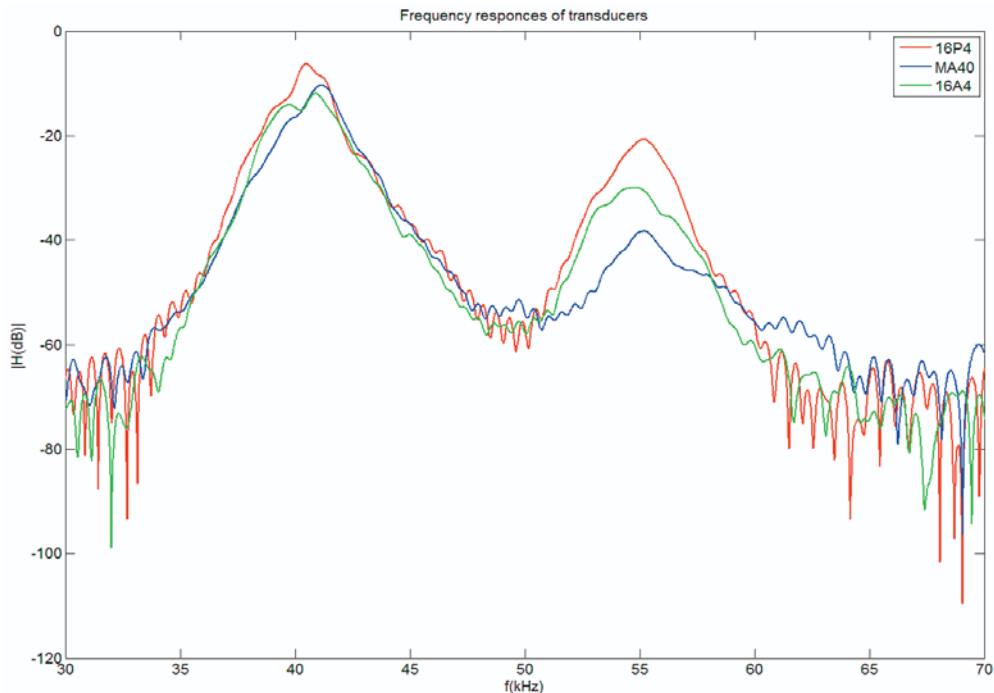
■ **Figure 3.** Setup to measure the sensibility of the transducers.

3.1. Study of transducers

The pre-selected transducers for the study were MA40S4R / S (Murata), MCUSD16P40B12R0 (Multicomp), MCUSD16A40S12R0 (Multicomp). All of them are ceramic piezoelectric transducers and are maneuverable, low cost and the resonance frequency is at 40 kHz.

In order to analyze which transducer is better, the layout showed in Figure 3 has been implemented. The frequency response of the transducers (equation 17) has been obtained as the ratio of the received signal $V_{rx}(f)$ of the evaluated transducer and the transmitted signal, $V_{tx}(f)$ (the transmission transducer was the same for all the measures). Different kind of signals were used (broadband signal and narrow band signals) and the analyzed bandwidth were between 30kHz and 70kHz. Figure 4 shows the results for the three preselected transducers. Although all of the transducers offered similar results, finally, the 16P4 model was chosen, since it showed the highest amplitude at the frequency of 40kHz with a 2.10kHz bandwidth.

$$H_{transducer}(f) = \frac{V_{rx}(f)}{V_{tx}(f)} \quad (17)$$



■ **Figure 4.** Modulus of frequency response of transducers.

The active area, the power and frequency of the carrier condition the application: larger area with low carrier NPS for meetings, high power for shorter environments.

3.2. Shape of the array and number of transducers

The correct configuration of the array depends on the application and the mounting space available in each case. As the generation length depends on the morphology of the array, different morphologies lead to different responses in audio frequency and directivities [3]. In Figure 5, we can see the different configurations.

We have two large groups: rectangular group in which we find to the arrangement matrix and hexagonal and circular group, in which we find the circular array and the ring. Finally, a hexagonal embodiment with a bee honeycomb distribution was chosen because it maximizes the active area respect to the others morphologies (circular or rectangular) [10].

On the other hand, to decide on the appropriate number of transducers, the authors assessed two aspects: budget and previous works [3,5][11][12]. Finally, the chosen number was 91, as it is a correct number for our parametric speaker.

3.3. Layout and assembly

As we have explained in the previous section, the selected morphology is hexagonal formed by 91 transducers, but we organized them by 4 independent rings around the central point instead of connecting all the transducers (91) in parallel. This fact leaves the doors open for future works as: the use of each ring with different voltage respect to the others, beamforming or the study of directivity depending on the active area.

The authors have tried that all the rings have similar number of transducers: the central ring 1 (that is a circular shape) has 19 transducers meanwhile the next rings (rings 2, 3 and 4) have 18, 24 and 30 respectively. In conclusion, with this configuration, speaker beam was made as uniform as possible (compensation of amplitude) and a phase compensation [3] could also be performed.

3.4. Design of the amplifier

For the amplification stage, the C.I. LM3886 was used [10] which offers the bandwidth necessary (20kHz – 60kHz) and the output power (68W) for the 91 transducers. Additionally, the existence of a lower pole will influence the frequency response of the loudspeaker, improving the lack of bass.

4. Results

In this section, the different experimentals that have been carried out are explained and the performance of the implemented PAA is described. Each experimental tries to assess different aspects, which are:

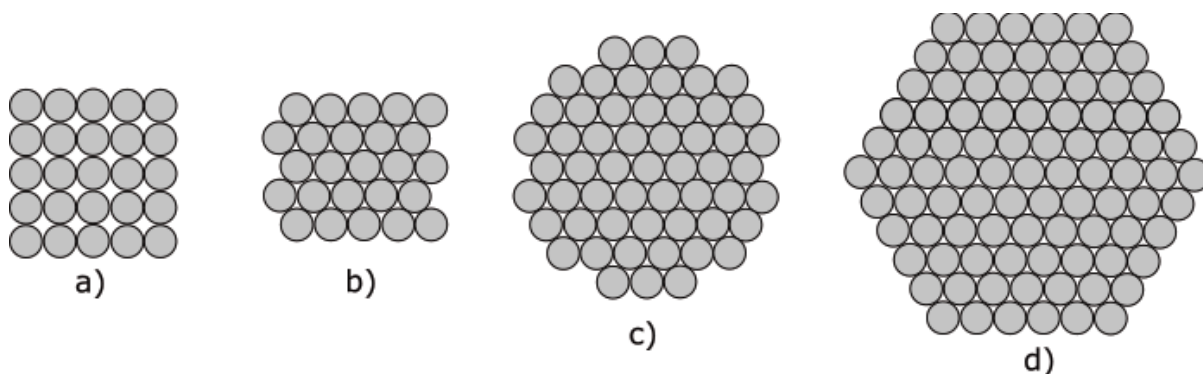


Figure 5. Different morphologies of array. a) Matricial. b) Uniform Hexagonal Array(UHA). c)Circular. d)Hexagonal.

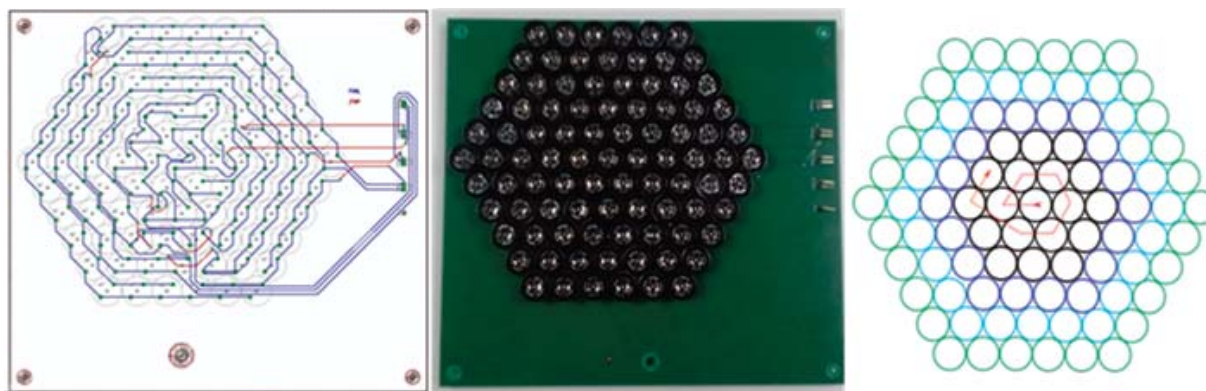


Figure 6. Left and center: implementation of the routing and result of the array. To the right: position the transducers with the clockwise direction marked by the red arrow. Circles of the same color denote transducers of the same ring, interconnected between them.

- Amplitude response of the loudspeakerThe pressure received as a function of the input voltage.
- Audible beam and ultrasonic frequency response.
- Radiation diagram of the audible beam and ultrasonic.
- Sweeping the carrier frequency of the system.

4.1. Amplitude response of the loudspeaker

This experiental asses how the PAA response to different amplitudes of the input signal, that means the dynamic range of the system. For this purpose, we set the receiver (Microphone ICP M5 PCB PIEZOTRÓNICS) one meter away from the loudspeaker and an amplitude modulation signal was emitted. The amplitude of the carrier signal was swept from 0.05 to $0.75V_p$ and was amplified 40 times by the amplifier ($2V$ to $30V$). The carrier frequency was $40kHz$, the modulation factor was 0.5 and the modulating signal was a sinousoidal signal of $1kHz$.

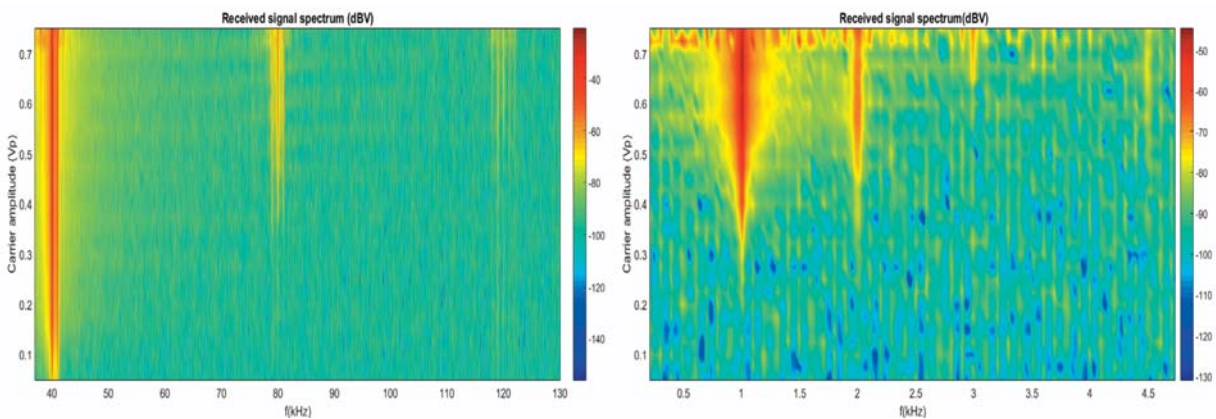
Figure 7 shows the received amplitude versus frequency (axis X) and versus transmitted amplitude (axis Y) for an ultrasound signal (Figure7a) and demodulated sound signal (Figure7b). We can notice that the maximum level of the main beam ($40kHz$) is reached with low level of signal ($0.2V$) (Figure 6a). When the input amplitude reach $0.35V$, we also

notice how other harmonics appear: $80kHz$, $80 \pm 1kHz$, $120kHz$, $120 \pm 1kHz$, etc. Meanwhile, in the audible tone we see how the level increases, until it reaches its maximum (input signal at $0.5V$). In this point, the level of the harmonics ($2kHz$ and $3kHz$) starts to be appreciable (Figure 6b).

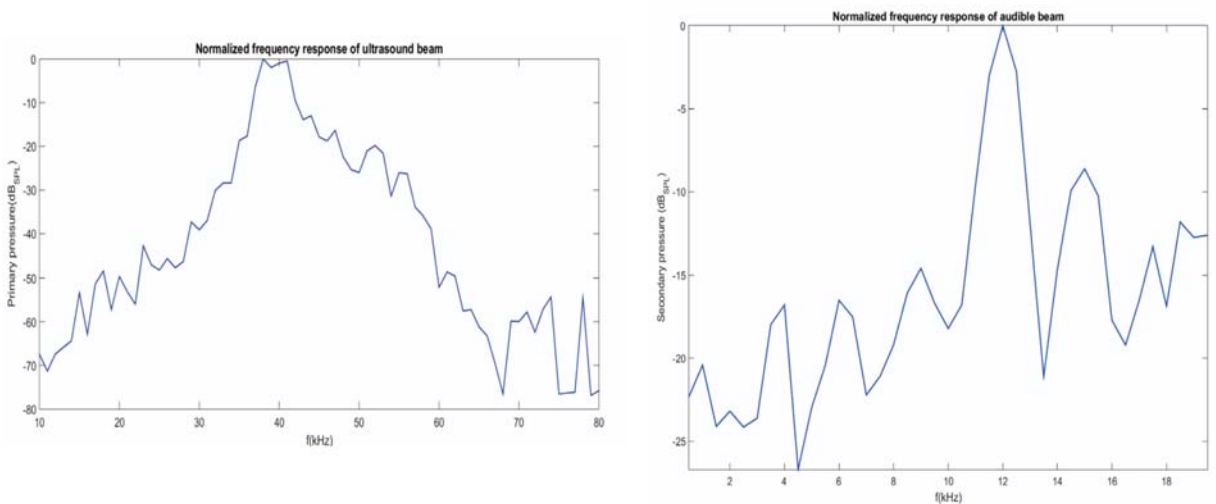
4.2. Frequency response of the loudspeaker

The aim of the next measure was to obtain the frequency response of the system. For this purpose, the layout was kept similar to the previous one (one meter between the transmitter and receiver) but we have to take into account that there are two beams: the primary one corresponding to the ultrasound one and the secondary one corresponding to the audible beam. Therefore, two different types of excitations or frequency swept were carried out. To measure the frequency response of the ultrasonic beam, we perform a frequency sweep with a pure sinusoidal signal from $10kHz$ to $80kHz$. Figure 8a represents the frequency sweep versus amplitude, where we have assumed that the ICP microphone M5 (receptor) has a flat response in the working bandwidth. In addition we can check that the maximum pressure level is obtained around $40kHz$, whose value was $123.3 dB_{SPL}$. The bandwidth of the ultrasonic beam at $-6dB$ was $4.6154kHz$.

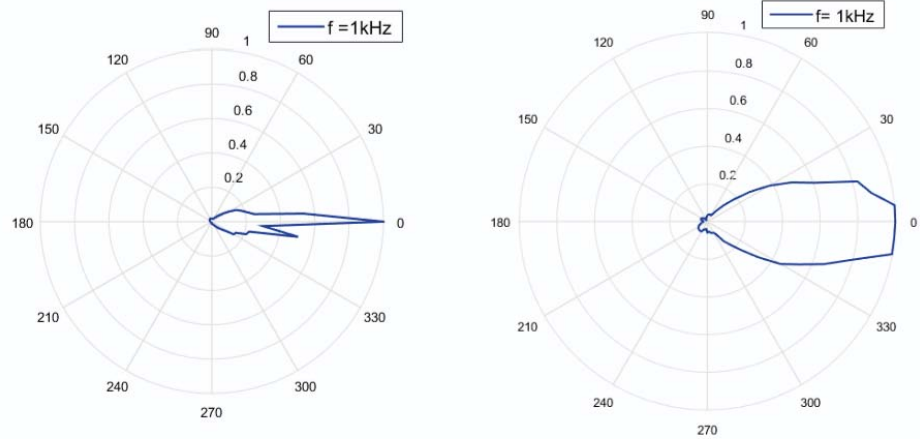
On the other hand, to measure the frequency response of the audible beam, we employed an AM signal where



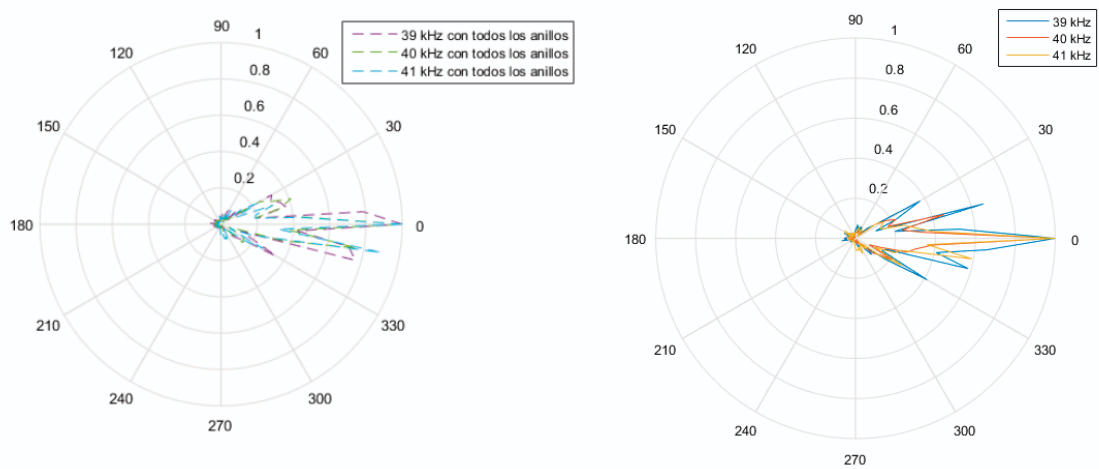
■ **Figure 7.** a) Received ultrasonic band, with modulated signal harmonics, b) Demodulated tone in receiver of $1kHz$ and their respective harmonics (first harmonic in $2kHz$).



■ **Figure 8.** Left: Normalized frequency response of the ultrasonic band. Right: standard frequency response of the audible band.



■ **Figure 9.** Left: 1kHz audible tone radiation pattern measured at 1m. Right: Audible tone radiation pattern of 1kHz measured at 2m.



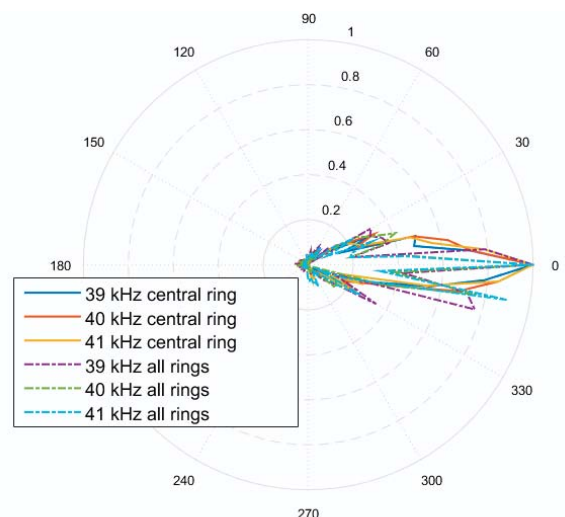
■ **Figure 10.** Left: Ultrasonic beam diagram at different frequencies at 1 meter. Right: Ultrasonic beam diagram at different frequencies at 2 meter.

we perform a frequency sweep of the modulating signal from 1kHz to 20kHz (Figure 8b). We observe that the maximum pressure is obtained for 12kHz and whose value is 85.52dB_{SPL} , a fairly considerable pressure level, taking into account the Wegel curve. The minimum sound pressure level is reached at 4.5kHz with a sound pressure level of 58.8dB_{SPL} . Therefore, we can notice that our speaker could be used for transmitting music or language, as far as levels of pressure and bandwidth are concerned.

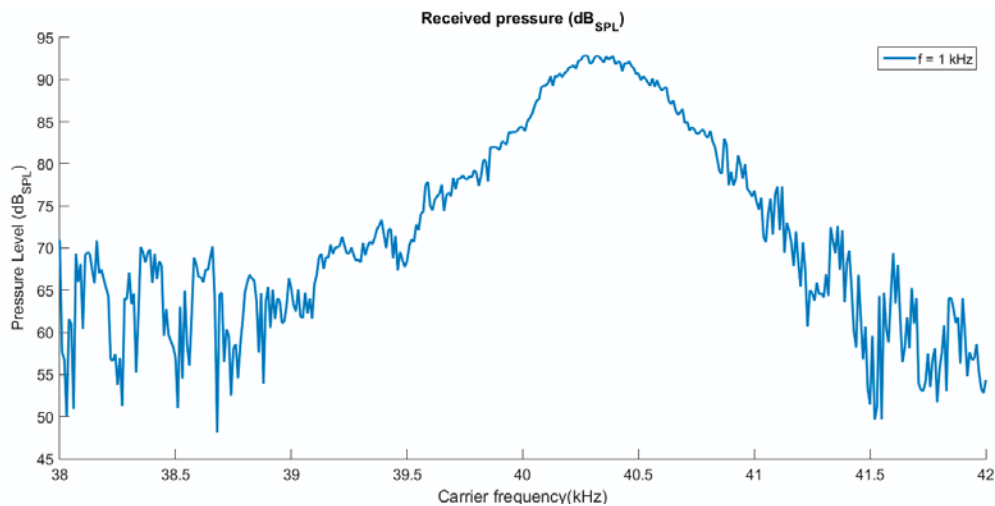
4.3. Radiation diagrams

In this section, the measurements of the radiation diagram are presented. The layout was kept similar to the previous one, but two different distances between loudspeaker and receiver were performed: 1 m and 2 m. The transmitter was turned from 0° to 360° in 5° steps (75 points), meanwhile the receiver was kept in the same position. Different receivers were used in the reception stage: a 16P4 transducer (for ultrasound beam), Beyerdynamic microphone (for sound beam) and M5 ICP (for redundancy as broadband receiver).

For the audible radiation diagram (Figure 9), all the rings were connected and the transmitted signal was an AM signal with 1kHz modulating signal. At one meter (Figure 9a), the audible beam width (4°) is much smaller than



■ **Figure 11.** Ultrasonic beam diagram at different frequencies for the center ring and all connected rings, measured at 1 meter; right: Ultrasonic beam diagram with all connected rings, measured at 2 meters.



■ **Figure 12.** Sound pressure of 1 kHz tone depending on carrier sweep.

two meters (Figure 9b) (25°). We also observe that as we move away in distance the beam width widens and the speaker is not as directive as originally expected.

For ultrasonic radiation diagram, (Figure 11), the two distances (1m and 2m) were kept for the analysis but a pure sinusoidal signal of different frequencies was used. Figure 11a and Figure 11b show as a higher frequency, as more directive. In addition, the authors have verified that the directivity increases as the number of transducers increases (Figure 11). Also to emphasize that our design is not exempt of secondary lobes, that must be grid lobes reduced by the stepped structure, as we have seen in the developed theory of the PAA. We can also see that the beam width does not depend as much on the distance as the audible beam.

4.4. Sweep of carrier frequency

To measure if the optimum frequency to work in our system, we perform a frequency sweep of the carrier frequency, keeping all other parameters constant. The maximum pressure value received was not at 40kHz as we can see in Figure 12 and it is slightly displaced towards higher frequencies, particularly it is in 40.27kHz , with a maximum sound pressure value of 92.84 dB SPL .

5. Conclusions

In this work, the theoretical fundament of the PAA has been explained: Rayleigh, absorption and generation distances and how the active surface of the PAA conditions it. Beginning from this study, a practical implementation of a PAA has been carried out. A hexagonal morphology has been selected to maximize the active surface respect to the number of the transducer. Finally, the empirical characteristics of the PAA have been presented: we have verified that two directional beams are created, ultrasonic one and audible one. The ultrasonic beam was more directive than the audible one, due to the higher frequencies. As for audible beam, the loudspeaker reaches acceptable levels for the reproduction of speech and music, as it has a considerable bandwidth.

With regard to directivity, which is one of the parameters with which we focus much on this project, we can say that indeed our speaker is very directive (4°) for short distances, close to one meter. It is no longer so much from two meters, where the beam width widens up to 25° .

Acknowledgement

Authors acknowledge support Spanish Administration under grant BIA2014-55311-C2-2-P.

References

- [1] J. G. Tylka, "On the Calculation of Full and Partial Directivity Indices," *Tech. report, Princet. Univ.*, pp. 1–12, 2014.
- [2] F. E. Toole, *Sound Reproduction: Loudspeakers and Rooms*. Elsevier, 2008.
- [3] D. Olszewski and K. Linhard, "Optimum array configuration for parametric ultrasound loudspeakers using standard emitters," *Proc. - IEEE Ultrason. Symp.*, vol. 1, pp. 657–660, 2006.
- [4] D. Olszewski, "Optimum Carrier Frequency for Ultrasound Loudspeaker," *Proc Symp. Ultrason. Electron.*, vol. 27, pp. 337–338, 2006.
- [5] P. Ji, C. Ye, and J. Tian, "Development of a directional loudspeaker system for sound reproduction," pp. 591–594, 2007.
- [6] W. S. Gan, J. Yang, and T. Kamakura, "A review of parametric acoustic array in air," *Appl. Acoust.*, vol. 73, no. 12, pp. 1211–1219, 2012.
- [7] J. J. Croft and J. O. Norris, "Theory, History, and the Advancement of Parametric Loudspeakers A TECHNOLOGY OVERVIEW," San Diego, CA, 2003.
- [8] M. . Hamilton and D. . Blackstock, *Non linear Acoustics*, 1st ed. San Diego, CA: Academic Press, 1998.
- [9] F. Farias and W. Abdulla, "On Rayleigh distance and absorption length of parametric loudspeakers," in *Proceedings of APSIPA Annual Summit and Conference*, 2015, vol. 2, no. December, pp. 1262–1265.
- [10] C. Gallardo Llopis, "Altavoz ultrasónico: sistema focalizado de sonido," Universidad Politécnica de Valencia, 2017.
- [11] Glenwood Garner III, "Design of Optimal Directional Parametric Acoustic Arrays in Air," 2011.
- [12] U. Sayin and O. Guasch, "Directivity control and efficiency of parametric loudspeakers with horns.," *J. Acoust. Soc. Am.*, vol. 134, no. 2, p. EL153-7, 2013.

Biographies



G. Lara was born in Valencia. He received the Ingeniero de Telecomunicación and the Doctor Ingeniero de Telecomunicación degrees from the Universidad Politécnica de Valencia (UPV) in 2010 and 2017 respectively.

His research interest is focused in signal processing for passive acoustic monitoring. Currently, he is involved in the development of a submarine buoy capable of recording underwater sounds without sample loss, programming the electronics, the internal hardware and embedding the developed algorithms.



Alicia Carrión received an MEng degree in Telecommunication Engineering from the Universitat Politècnica de València (UPV), Spain, in 2011. Her MSc work was carried out at Fraunhofer Institute IOSB, Karlsruhe, Germany. Currently, she is a PhD student at the Institute of Telecommunication and Multimedia

Applications (ITEAM) of UPV, Spain. Her research interests include nonlinear signal processing and signal modality characterisation, with applications in submarine acoustics, ultrasonic testing, and finance.



Dr. Jorge Gosálbez was born in Valencia (Spain) in 1975. He received the Ingeniero de Telecomunicación and the Doctor Ingeniero de Telecomunicación degrees from the Universidad Politécnica de Valencia (UPV) in 2000 and 2004 respectively. He is Assistant Professor at

Departamento de Comunicaciones (UPV) and member of the Signal Processing Group of the Institute of Telecommunication and Multimedia Applications (I-TEAM) of UPV.

His research concentrates in the statistical signal processing area, where he has worked in different theoretical and applied problems, many of them under contract with the industry. His theoretical aspects of interest are time-frequency analysis, signal detection and array processing. Currently he is involved in ultrasound signal processing for non-destructive evaluation of materials, in surveillance systems based on acoustic information and in acoustic source location and tracking based on sensor and array signal processing. He has published more than 50 papers including journals and conference contributions and has been involved in more than 30 competitive research projects (4 EU) and more than 10 contracts with enterprises, most of them related with signal processing and nondestructive evaluation.



Guillermo Pérez Torró, born in Alcoi (1992), received his B.Sc. degree in Telecommunications Engineering and M.Sc. degree in Telecommunication Systems and Networks in the Universitat Politècnica de València (UPV) in 2015 and 2016 respectively. As a part of his B.Sc. thesis, he developed, in

collaboration with the Grupo de Investigación Biomédica de Imagen (GIBI) of the Hospital Universitario y Politécnico La Fe (HUPLF) of Valencia, a medical image processing application to quantify hemodynamic parameters. Finished his M.Sc. degree, he began working as an associate researcher in the Grupo de Tratamiento de señal (GTS) of Instituto de Telecomunicaciones y Aplicaciones Multimedia (ITEAM), involved in areas of material characterization with acoustic and ultrasonic non-destructive techniques. His main interests are signal statistical processing and pattern recognition to assess material dynamic properties.



R. Miralles was born in Valencia (Spain) in 1971. He received the degree of Ingeniero de Telecomunicación and the Ph.D. in Telecomunicación from the Universitat Politècnica de València (UPV) in 1995 and 2000 respectively. In 1996 he became a lecturer in the Departamento de Comunicaciones

at the Escuela Politécnica Superior de Gandía. From 2000 until now he has been working as an Assistant Professor in the Escuela Técnica Superior de Ingenieros de Telecomunicación (Valencia). He is member of the management team of the Institute of Telecommunication and Multimedia Applications (ITEAM).

His research interests are mainly focused on signal processing for non destructive testing, marine bioacoustics signal processing, data mining, recurrence plots, surrogate data, nonlinear detection/ characterization and time frequency analysis. He has published more than 80 papers in these areas including journals and conference communications.



Santiago Vázquez was born in Valencia (Spain). He received the Telecommunication Engineering degree from the Universidad Politécnica de Valencia (UPV) in 2015. He has been awarded with the First Prize for the Best Final Degree Project of the College of Telecommunications Engineers of

Comunidad Valenciana (COITCV) in 2016. Currently, he is working towards the Ph. D. with a FPI fellowship from the Spanish government in the Institute of Telecommunication and Multimedia Applications (ITEAM) of UPV. His research interests include signal and image processing applied in ultrasonic signals and biomedical data.



Ignacio Bosch was born in Valencia (Spain) in 1975. He received Telecommunications Engineering and PhD degrees from the Universidad Politécnica de Valencia (UPV) in 2001 and 2005 respectively. In 2004 he became a lecturer in the Departamento de Comunicaciones (UPV). From 2006 until now he has

been working as an Assistant Professor at the Escuela Técnica Superior de Telecomunicaciones de Valencia (UPV). He is member of the Signal Processing Group of the Institute of Telecommunication and Multimedia Applications (I-TEAM) of UPV. He is responsible of developing algorithms and systems for infrared signal processing surveillance and image processing for biomedical applications. His research interests are signal processing applications for ultrasonic systems in non-destructive evaluation, infrared signal processing for automatic fire detection and image processing and applications in biomedical problems. He has been actively participating in more than 48 research projects and/or research contracts. He has published more than 90 papers including journals and conference contributions.



Carles Gallardo Llopis was born in Gandia(Spain). He received the Telecommunication Engineering degree from the Universidad Politécnica de Valencia (UPV) in 2016. Currently, he is a PhD student at the Institute of Telecommunication and Multimedia Applications (I-TEAM) of UPV. His

research interests are ultrasonic tomography as a NDT and his applications on cementitious materials and reconstruction algorithms.